RSC Advances

PAPER

View Article Online
View Journal | View Issue

Cite this: *RSC Adv.*, 2020, **10**, 6185

Constructing an ultra-adsorbent based on the porous organic molecules of noria for the highly efficient adsorption of cationic dyes†

Danyong Jiang,[a] Ruiping Deng,[c] Gang Li,[a] Guoli Zheng *[a] and Huadong Guo *[b]

Received 17th October 2019
Accepted 22nd January 2020

DOI: 10.1039/c9ra08490h

rsc.li/rsc-advances

A novel Noria-POP-1 material has been successfully synthesized by the simple polymerization of the porous organic molecules of noria and aryl diamines. Noria-POP-1 displayed excellent adsorption capacity for cationic dyes from water with selective removal ability. The adsorption experiments show that Noria-POP-1 displays a remarkable capability to selectively adsorb and separate methylene blue with an adsorption capacity of 2434 mg g^{-1}, which is the highest value obtained so far for porous organic polymers.

Introduction

Organic dyes have been paid attention because of their wide applications in textiles, medicine, and paper and printing industries, which is causing negative effects on the environment and human health. Currently, many methods are applied to remove dye pollutants, such as photocatalytic degradation,[1] membrane separation,[2,3] electrochemical methods[4] and adsorption.[5–9] Comparatively, adsorption using porous materials is the most effective method to remove organic dye pollutants with the advantages of simple operation, low cost and fast speed.[3] The use of traditional adsorbents such as zeolites and activated carbons is restricted because of their poor selective adsorption, low adsorption capacity and weak regeneration ability. Therefore, various porous materials with high surface areas and tunable skeletons for dye adsorption have been reported such as porous organic polymers (POPs)[10–23] and metal–organic frameworks (MOFs).[24–29] Although MOFs have the advantages of rapid adsorption kinetics and high saturation capacities, they still suffer from the drawbacks of water stability in practical applications because of their labile metal–organic coordination bonds, which can even be a potential source of metal ion contamination. Compared with MOFs, POPs without metal ions are constructed by covalent bonds and display good chemical stability. Thus, POPs are considered to be good candidates for dye removal from wastewater. Although POPs have made great progress, the synthesis of new POPs with high adsorption capacity and fast adsorption kinetics for dye removal is still an attractive but challenging task.

Recently, porous organic molecules (POMs)[30–36] with intrinsic porosity have been reported as excellent candidates for separation,[37–45] and they can be used as a host for guest molecules. Unlike materials with extended networks and frameworks, POMs have no covalent bonds between isolated molecules. POMs are usually soluble in common solvents, which leads to difficulties in their separation and recycling. To the best of our knowledge, the effective way to improve the adsorption capacity of adsorbents is through an increment in the adsorption sites. Therefore, we believe that new POP materials with dye adsorption can be produced by the polymerization of porous organic molecules and other monomeric moieties. Bearing the above-mentioned consideration in mind, we have rationally fabricated Noria-POP-1 *via* the diazo-coupling reaction of aryl diamines with noria (Fig. 1).[46] In this paper, we chose noria as one of the monomeric moieties based on the following considerations: (1) according to previously reported studies, noria can be easily synthesized in water, and the raw materials for preparing noria are cheap and easy to obtain;[36] (2) noria has a double-cyclic ladder-like structure with twenty-four hydroxyl groups, six cavities on the side, and a large hydrophobic central hole, due to which it can be used as a host for dyes; (3) recently, hierarchically porous phenolic azopolymers with free phenolic hydroxyl groups have been reported with good adsorption capacity for dyes, which indicates that Noria-POP-1 can be a potential dye adsorption material.[21,46]

Herein, we synthesized Noria-POP-1 in an aqueous solution without any template under mild conditions. Although numerous POPs have been reported for dye adsorption, very few POPs based on porous organic molecules have been reported. Recently, Trabolsi and co-workers reported a rich porous covalent polycalix[4]arene material with the maximum adsorption capacities of 625 and 484 mg g^{-1} for cationic organic methylene blue (MB) and rhodamine B (RhB) dyes, respectively.[47] In our

[a]*Key Laboratory of Catalysis and Energy Materials Chemistry of Ministry of Education, Hubei Key Laboratory of Catalysis and Materials Science, South-Central University for Nationalities, Wuhan 430074, China. E-mail: zhengguoli2002@aliyun.com*

[b]*Department of Chemistry, Changchun Normal University, Changchun, 130032, P. R. China. E-mail: hdxmguo@163.com*

[c]*Changchun Institute of Applied Chemistry, Chinese Academy of Sciences, State Key Laboratory of Rare Earth Resource Utilization, China*

† Electronic supplementary information (ESI) available. See DOI: 10.1039/c9ra08490h

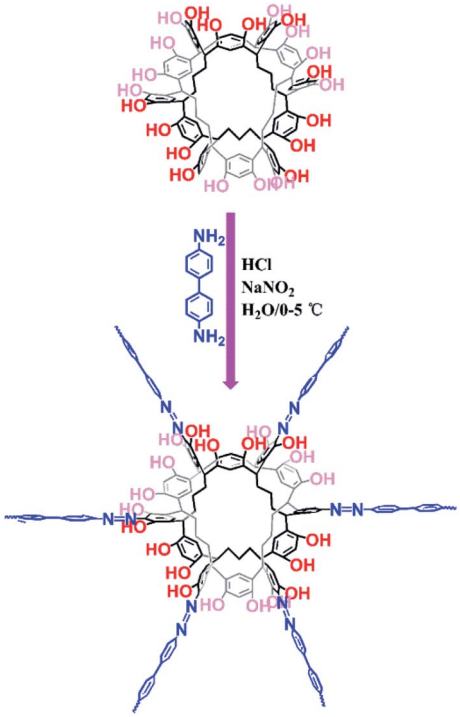

Fig. 1 A schematic showing the synthesis of Noria-POP-1.

work, Noria-POP-1 displayed excellent adsorption capacity for MB, and its selective dye removal ability was owing to a large conjugated structure and abundant phenolic hydroxyl groups. The adsorption capacity for MB is up to 2434 mg g^{-1}, which is the highest value obtained for POPs so far. Isothermal adsorption analysis and kinetic analysis were carried out to study the adsorption mechanism. The adsorption process for methylene blue was very fast and could be completed in 2 min. In addition, the adsorption capacities for rhodamine B (RhB) and neutral red (NR) are better than most reported results. Since Noria-POP-1 has high capacity, good stability and easy regeneration, we anticipate that this new type of POP porous material will hold great promise for the removal of dye contaminants from polluted water.

Experimental

Materials and equipment

All reagents were commercial products of high purity and were not further purified except noria, which was prepared according to a previously reported method.[48] Fourier transform infrared (FT-IR) spectra were measured in the 4000–400 cm^{-1} wavenumber range using a PerkinElmer model 580B IR spectrophotometer with the KBr pellet technique. Thermogravimetric analysis (TGA) was performed on an SDT2960 analyzer (Shimadzu, Japan) up to 750 °C at a heating rate of 10 °C min^{-1} under N_2. UV-Vis spectra were recorded on Agilent 8453. The solid-state ^{13}C cross-polarization/magic angle spinning nuclear magnetic resonance (^{13}C CP/MAS) NMR spectrum was recorded on a Bruker SBAvance III 500 MHz spectrometer. Field-emission scanning electron microscopy (SEM) was performed on a JEOL JSM-7800F microscope under an accelerating scanning voltage of 3.0 kV. Surface area and pore size distribution of Noria-POP-1 were measured using nitrogen adsorption and desorption at 77 K on a Micromeritics ASAP2020 volumetric adsorption analyzer.

Synthesis of Noria-POP-1

The preparation of Noria-POP-1 requires two steps. First, 4,4′-diaminobiphenyl (3 mmol) was added to a 500 ml round-bottomed flask charged with 100 ml of deionized water and 1.5 ml of concentrated hydrochloric acid. Then the mixture was stirred for 15 min under ice bath conditions; next, 30 ml of aqueous solution of sodium nitrite (6.1 mmol) was added and stirred for 30 min to completely convert the amino groups into diazonium salts. Subsequently, the mixture was adjusted to neutral pH by adding a dilute solution of Na_2CO_3 and then mixed with 100 ml of an aqueous solution of noria (1 mmol) and Na_2CO_3 (12 mmol) at 0–5 °C. After reacting for 24 hours, the mixture was filtered, and the residue was washed with deionized water, methanol and THF and then dried under vacuum at 80 °C for 12 hours.

Organic dye adsorption

The adsorption of dyes on Noria-POP-1 was carried out by immersing 10 mg of Noria-POP-1 into a 20 ml solution containing different concentrations of MO, AR1, MB, RhB and NR. The concentration of the dye solution was measured by a UV-Vis spectrophotometer. All experiments were carried out in triplicate under the same conditions.

Effect of pH

In order to investigate the effect of pH on the adsorption of dyes by Noria-POP-1, 10 mg of Noria-POP-1 was immersed in 20 ml solution containing MB, RhB, and NR at different pH values and stirred at room temperature for 24 hours (Noria-POP-1 was stirred at room temperature for 6 hours while adsorbing the MB solution at pH = 12). The pH of the solution was adjusted using hydrochloric acid and sodium hydroxide.

Maximum adsorption amount experiment

The maximum adsorption amounts of MB and RhB were measured at pH = 12. In a typical experiment, 10 mg of Noria-POP-1 was soaked into a 20 ml solution containing different concentrations of MB and RhB and stirred at room temperature for 6 hours. The NR maximum adsorption amount was measured using the same method at pH = 7. The concentration of the dye solution was measured by a UV-Vis spectrophotometer.

Adsorption kinetics

The adsorption experiments were carried out as follows: 10 mg of Noria-POP-1 was added to an aqueous solution of MB, RhB and NR (20 ml, 50 ppm). Then, the mixture was stirred at room temperature. The concentrations of the dyes at different time intervals were monitored by a UV-Vis spectrophotometer.

Selective adsorption

An aqueous solution of MB (10 ml, 100 ppm) was mixed with MO, AR1, and RhB (10 ml, 100 ppm) and stirred at room temperature for 20 min. Then, we removed Noria-POP-1 from the mixed solution by centrifugation. The supernatant was analyzed using a UV-Vis spectrophotometer.

Desorption experiments and reusability

Ten mg of Noria-POP-1 was immersed in a 20 ml aqueous solution of MB with pH = 12 and stirred 6 h. Then, the mixture was centrifuged and the supernatant was collected; the concentration of the dye in the solution was estimated by using a UV-Vis spectrophotometer. The release of MB from Noria-POP-1 was achieved by soaking the sorbents in an ethanol solution of hydrochloric acid (0.1 mM). Then, the samples were dried under vacuum at 80 °C for 12 h for the next cycle experiment.

Results and discussion

The reaction of noria and 4,4′-diaminobiphenyl at a molar ratio of 1 : 3 in water at 0–5 °C afforded a black powder of Noria-POP-1 with a high yield of 82%. The obtained Noria-POP-1 was insoluble in any organic solvent. The synthesized Noria-POP-1 was characterized by solid-state cross-polarization magic angle spinning (CP/MAS) ^{13}C NMR spectroscopy and Fourier-transform infrared (FT-IR) spectroscopy. The ^{13}C NMR spectrum of Noria-POP-1 is shown in Fig. 2. As expected, two types of carbon signals are observed. The signals in the range from 104 to 153 ppm are attributed to the aromatic carbons of Noria-POP-1. Additionally, the weak signals at around 26–49 ppm correspond to the methylene carbon atoms of Noria-POP-1. In the FT-IR spectrum of Noria-POP-1, the asymmetric stretching vibration characteristic peak of the –N=N–double bond appears at around 1390 cm^{-1} (Fig. S2 and S3†). The broad absorption peak at around 3416 cm^{-1} is attributed to the –OH stretching vibration, confirming the successful coupling reaction. TGA analysis was carried out to study the thermal stability of Noria-POP-1, and the results indicated that Noria-POP-1 could be thermally stable up to 246 °C (Fig. S4†). Above 246 °C, the weight loss was attributed to the decomposition of the framework. The first weight loss (10.2%) was around 112 °C, which was assigned to the weight loss of the solvent. As shown in Fig. S5†, Noria-POP-1 demonstrates strong and broad absorption peaks in the UV-Vis range from 200 to 800 nm, indicating its potential application in photocatalysis.

As shown in Fig. 3, the morphology of Noria-POP-1 is determined by scanning electron microscopy (SEM) and transmission electron microscopy (TEM). The SEM image shows that Noria-POP-1 is composed of irregularly shaped tiny particles. Energy dispersive X-ray (EDX) analysis was carried out to determine the elemental composition of the material (Fig. S6 and Table S3†).

The porosity information was obtained by nitrogen adsorption–desorption measurements at 77 K. Noria-POP-1 exhibited type IV isotherms with low porosity, indicating the existence of macropores between the particles. The BET surface area of Noria-POP-1 was 1.8 m^2 g^{-1}, the pore size was 70 nm, and the pore volume was 0.032 cm^3 g^{-1} (Fig. S7†). It was interesting to compare Noria-POP-1 with previously reported HAzo-POPs synthesized from tri/diphenols and 4,4′-diaminobiphenyl.[21,46] The common characteristic in both the materials is that both the polymers have been synthesized based on a diazo-coupling reaction without any template. Although the BET surface area and pore volume of Noria-POP-1 were lower than those for HAzo-POPs, the adsorption capacity of Noria-POP-1 for MB was considerably higher than that of HAzo-POPs.

The as-prepared Noria-POP-1 was a jelly-like solid. After vacuum drying and dehydration, the volume was drastically reduced and it became a hard blocky solid, suggesting that the pores of Noria-POP-1 shrank after dehydration. Recently, a few nonporous organic solids with remarkable sorption behaviour have been reported as 'frustrated organic solids', which have been synthesized by removing the solvent molecules from the structure. During the desolvation process, new porous materials were formed, which could rapidly adsorb gases.[43,48–50] Inspired by the frustrated organic solids, we reason that the pores within Noria-POP-1 were reformed during the process of going from a desolvated form to a solvated form by absorbing water molecules.

The above-mentioned results prove that water molecules can form hydrogen bonds *via* –OH, supporting the pore structure. The pores of Noria-POP-1 shrink and expand when it loses or absorbs water, which may be the reason Noria-POP-1 with a low BET surface area exhibits excellent dye adsorption. All these results show that POPs constructed from POMs (noria) have greater flexibility and adsorption capacity.

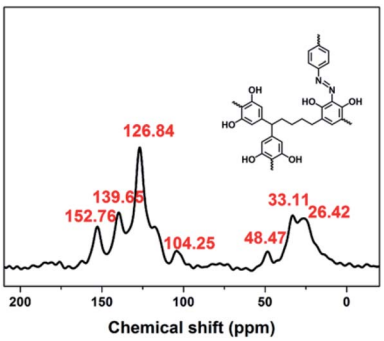

Fig. 2 The solid-state ^{13}C-CP/MAS NMR spectrum of Noria-POP-1.

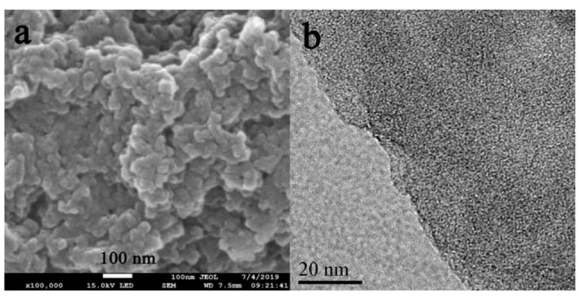

Fig. 3 (a) The SEM image of Noria-POP-1; (b) the TEM image of Noria-POP-1.

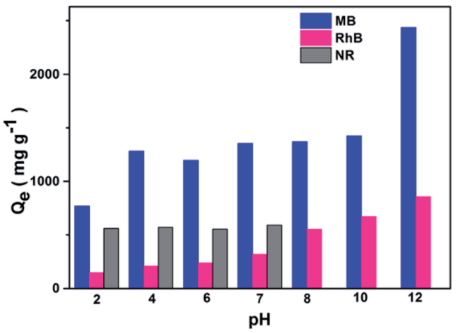

Fig. 4 Adsorption performance of Noria-POP-1 for dyes (MB, RhB, and NR) at different pH values.

In order to elucidate the adsorption mechanism, five different dyes (*i.e.*, methyl orange (MO), acid red 1 (AR1), rhodamine B (RhB), methylene blue (MB) and neutral red (NR)) with different sizes and charges were used to study the performance of Noria-POP-1 as an adsorbent (Fig. 1). In the adsorption experiment, the adsorption capacities were calculated based on the UV-Vis spectra of the supernatants. Noria-POP-1 displayed selective affinity toward cationic dyes (MB and RhB) and neutral dye (NR), especially MB. Noria-POP-1 due to the negative charges could not adsorb anionic dyes (MO and AR1) at pH = 7. When the powder of Noria-POP-1 was added to the aqueous solutions of anionic dyes (MO and AR1), the color of the anionic solutions remained the same even after 20 minutes. The UV-Vis spectral results were consistent with the color observations (Fig. S8 and S9†). These results indicate that Noria-POP-1 can selectively adsorb cationic dyes, which was also confirmed through selective adsorption experiments (Fig. 7). The adsorption mechanism of cationic dyes likely involves electrostatic interactions between Noria-POP-1 and the dye molecules.

The adsorption capacities of Noria-POP-1 for dyes at different pH values were investigated. The initial pH value can not only change the surface charge of the adsorbent, but also ionize the dyes. As shown in Fig. 4, the adsorption capacities of Noria-POP-1 for MB and RhB increase with the increase in pH (2.0–12.0), indicating that the adsorption of MB and RhB on Noria-POP-1 is pH-dependent. On increasing the pH value, the surface of Noria-POP-1 gains a more negative charge. For the adsorption at pH = 7, the adsorption capacity of Noria-POP-1 for NR is 590 mg g^{-1}, which is much lower than the adsorption capacity of Noria-POP-1 for MB (1353 mg g^{-1}). In an alkaline environment, NR is unstable; therefore, we did not measure the adsorption capacities above pH = 7 (Fig. 4). As we know, neutral NR and cationic MB have similar structures and sizes, which indicate that electrostatic interactions contribute to the selective adsorption of MB over NR.

At pH = 12, the adsorption capacities of Noria-POP-1 for MB and RhB were the best and could reach 2434 and 855 mg g^{-1}, respectively. The experimental adsorption capacity of Noria-POP-1 for MB reached up to 2434 mg g^{-1}; as far as we know, this is the highest value for POPs reported so far (Table S4†). The ability of Noria-POP-1 to adsorb cationic MB is better than that for cationic RhB because RhB has a larger size than MB, which indicates that the pores formed after water absorption are more favorable for the adsorption of MB. All the results demonstrate that the excellent adsorption capacity of Noria-POP-1 for MB results from not only electrostatic interactions, but also spatial selectivity.

To determine the adsorption capacity of Noria-POP-1 for MB, NR and RhB, the adsorption isotherms of MB and RhB on Noria-POP-1 were obtained at room temperature. Fig. 5a shows that the adsorption capacity of Noria-POP-1 increases gradually on increasing the initial concentrations of MB, NR and RhB until reaching a plateau at $C_0 = 2200$ ppm for MB, $C_0 = 450$ ppm for NR, and $C_0 = 1600$ ppm for RhB. In order to reveal the adsorption isotherm mechanism, the adsorption isotherms were studied using the Langmuir isotherm model and Freundlich isotherm model (see ESI†). The fitting lines of the Langmuir and Freundlich isotherms are shown in Fig. 5b and S10,† respectively. The correlation coefficients in the case of the Langmuir isotherm model and the Freundlich isotherm model are shown in Table S1.† The results showed that the linear correlation coefficient of the Langmuir isotherm was higher than that of the Freundlich isotherm. The linear correlation coefficients (R_L^2) of MB, NR and RhB were 0.9999, 0.9981, and 0.9984, respectively. These results indicated that the adsorption of MB, RhB and NR on Noria-POP-1 was monolayer adsorption.

Adsorption kinetics is necessary to assess adsorption performance. Herein, the MB dye was selected as a typical sample. As shown in Fig. 6a, MB can be efficiently adsorbed by Noria-POP-1 within 3 minutes at pH = 12. All the experimental data were fitted with the pseudo-first-order and pseudo-second-order equations (see ESI†). The correlation coefficients of the

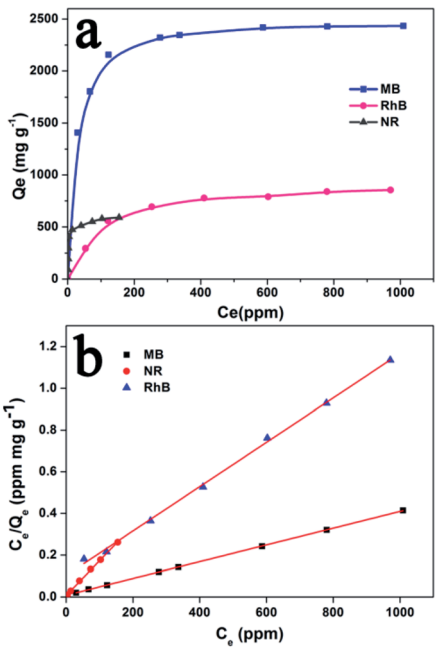

Fig. 5 (a) Adsorption isotherms of Noria-POP-1 for MB (pH = 12), RhB (pH = 12), and NR (pH = 7); (b) Langmuir isotherm models of MB, RhB, and NR on Noria-POP-1.

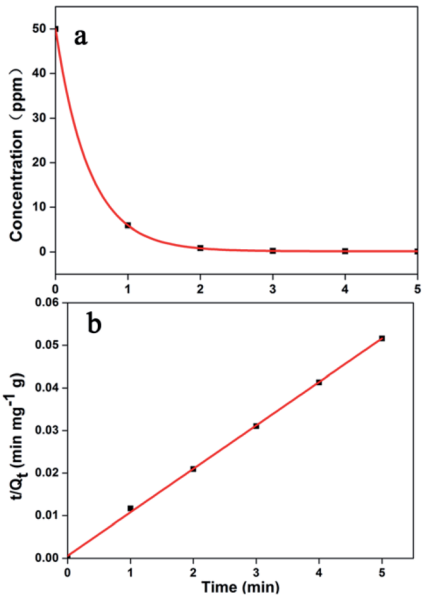

Fig. 6 (a) The effect of contact time on the removal of MB; (b) the pseudo-second-order model of Noria-POP-1 for MB.

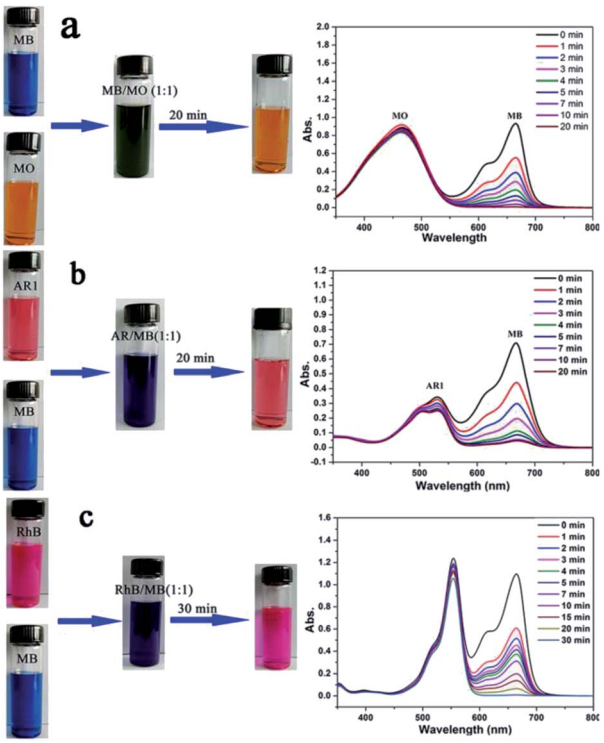

Fig. 7 Photographs and UV/Vis spectra of dye adsorption for evaluating the selective adsorption capability of Noria-POP-1 toward MB from mixed dyes: (a) MO and MB (solution: 100 ppm), (b) AR1 and MO (solution: 100 ppm); (c) RhB and MB (solution: 100 ppm).

pseudo-first-order and pseudo-second-order equations are shown in Table S2.† The results show that the adsorption of dyes has a good linear relationship with the pseudo-second-order kinetic model (Fig. S11–S15†). The linear correlation coefficients (R^2) of MB, NR and RhB were 0.9992, 0.9990, and 0.9960, respectively. The adsorption kinetic curves of the RhB (at pH = 12) and NR (at pH = 7) dye solutions are shown in Fig. S16 and S17,† respectively. The adsorption equilibrium times for MB, NR and RhB are 2, 30, and 240 min, respectively. The adsorption process of RhB was the slowest compared to other adsorption processes, which showed that the adsorption rate of Noria-POP-1 was dependent on the size of the guest molecules. These experiments indicate that the pores of Noria-POP-1 need more time to become larger after water absorption so as to be suitable for RhB adsorption.

The results of adsorption isotherms and adsorption kinetics prove that Noria-POP-1 has excellent adsorption capacity and fast adsorption toward MB. In order to show its potential application for MB adsorption in industries, we fabricated a simple adsorption device (Fig. S18†) and recorded a video (see the ESI video file†), which showed that MB was immediately adsorbed when the MB solution was filtered through this simple device.

The competitive adsorption and separation of dyes were also performed to investigate the selective adsorption ability of Noria-POP-1 for MB. Fig. 7 shows that Noria-POP-1 can efficiently separate MB from anionic dyes, which indicates that MO and AR1 have no effect on the removal of MB. In the mixture of MB and AR1, the decrease in the absorption peak at 530 nm is due to the adsorption of MB by Noria-POP-1 (Fig. 7b and S19†). Noria-POP-1 can selectively separate MB from MO or AR1, which proves that the main reason for the selective adsorption of MB from the MO and AR1 mixture should be electrostatic interaction. To further explore the selective adsorption of Noria-POP-1, the experiments of selectively adsorbing MB and RhB were carried out (Fig. 7c). The selective adsorption of MB from the RhB mixture may be partly attributed to the pores of noria. The pores of Noria-POP-1 were not enough to accommodate RhB, which reduced the adsorption capacity and adsorption speed of Noria-POP-1 for RhB. The competitive adsorption and separation experiments indicated that the pores of noria were also very important for the adsorption of dyes.

As Noria-POP-1 displayed excellent adsorption capacity for the cationic organic dye MB and good stability in water, regeneration experiments were carried out. The reusability of Noria-POP-1 is very important for industrial applications. The regeneration of Noria-POP-1 can be realized by the desorption of MB in an acidic methanol solution and the subsequent centrifugal separation. As shown in Fig. 8, the adsorption capacity of the regenerated Noria-POP-1 does not decrease significantly and is still 2068 mg g^{-1} even after five regeneration cycles. We speculate that the slight decrease in the adsorption capacity during the recycling experiment can be attributed to the residual MB dye in Noria-POP-1. All the results prove that the sorbent has good regeneration properties and stability.

Very recently, a new boron organic supramolecular framework with high adsorption capacity (3250 mg g^{-1} and 1388 mg g^{-1} for MB and RhB, respectively) has been reported by the Zhang group.[51] As far as we know, the adsorption capacity of Noria-POP-1 for MB is second only to that of the boron framework. Although

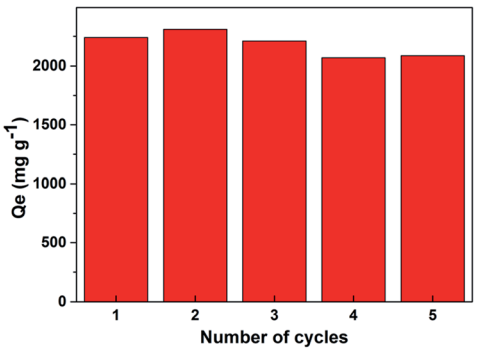

Fig. 8 Adsorption cycle performance of Noria-POP-1 for MB.

Noria-POP-1 has lower adsorption capacity than the boron framework, the raw materials used for the preparation of Noria-POP-1 are cheaper, which enables its large-scale production in industries. Meanwhile, the adsorption rate of Noria-POP-1 is much faster than that for the boron framework. Another disadvantage of the boron framework is that it may cause secondary pollution during the removal of dyes from water due to a large amount of boron inside the framework.

Conclusions

In conclusion, a novel Noria-POP-1 material has been successfully synthesized by the simple polymerization of noria and aryl diamines. This result indicates that new POP materials can be expected by polymerizing noria with various aromatic polyamines. The adsorption experiments show that Noria-POP-1 displays remarkable capability to selectively adsorb and separate the MB dye; the adsorption capacity is 2434 mg g^{-1}, and this is among the highest values for POPs reported so far. More importantly, the adsorption process for MB is very fast and Noria-POP-1 can be reused with good adsorption capacity (2068 mg g^{-1}) even after five cycles, which shows that Noria-POP-1 has great potential applications in removing organic dye pollutants from wastewater. In addition, the adsorption capacities for RhB and NR are 855 mg g^{-1} and 590 mg g^{-1}, respectively. The excellent performance of Noria-POP-1 provides an effective strategy for the synthesis of new dye adsorbents, which affords numerous possibilities for using various POMs as the building units with a view to accessing more POP materials for dye adsorption. All these studies are underway in our lab and will be reported in the future.

Conflicts of interest

There are no conflicts to declare.

Acknowledgements

The authors are grateful to the financial aid from the Jilin Natural Science Foundation of China (No. 20160414031GH) and National Natural Science Foundation of China (Grant No. 21201051, No.51502285).

Notes and references

1 C. Yu, Z. Wu, R. Liu, D. D. Dionysiou, K. Yang, C. Wang and H. Liu, *Appl. Catal., B*, 2017, **209**, 1–11.
2 R. Zhao, Y. Wang, X. Li, B. Sun and C. Wang, *ACS Appl. Mater. Interfaces*, 2015, **7**, 26649–26657.
3 H. Fan, J. Gu, H. Meng, A. Knebel and J. Caro, *Angew. Chem., Int. Ed.*, 2018, **57**, 4083–4087.
4 E. Brillas and C. A. Martinez-Huitle, *Appl. Catal., B*, 2015, **166**, 603–643.
5 C. Santhosh, V. Velmurugan, G. Jacob, S. K. Jeong, A. N. Grace and A. Bhatnagar, *Chem. Eng. J.*, 2016, **306**, 1116–1137.
6 H. Yan, H. Yang, A. Li and R. Cheng, *Chem. Eng. J.*, 2016, **284**, 1397–1405.
7 W. Yao, S. Yu, J. Wang, Y. Zou, S. Lu, Y. Ai, N. S. Alharbi, A. Alsaedi, T. Hayat and X. Wang, *Chem. Eng. J.*, 2017, **307**, 476–486.
8 Y. Guo, R. Wang, P. Wang, L. Rao and C. Wang, *ACS Sustainable Chem. Eng.*, 2019, **7**, 5727–5741.
9 M. C. Kimling, D. Chen and R. A. Caruso, *J. Mater. Chem. A*, 2015, **3**, 3768–3776.
10 H. Liua, R. Suna, S. Fenga, D. Wang and H. Liu, *Chem. Eng. J.*, 2019, **359**, 436–445.
11 S. Luo, Q. Zhang, Y. Zhang and P. Kevin, *ACS Appl. Mater. Interfaces*, 2018, **10**, 15174–15182.
12 Y. Huang, G. Ruan, Y. Ruan, W. Zhang, X. Li, F. Du, C. Hu and J. Li, *RSC Adv.*, 2018, **8**, 13417–13422.
13 M. Zhou, T. Wang, Z. He, Y. Xu, W. Yu, B. Shi and K. Huang, *ACS Sustainable Chem. Eng.*, 2019, **7**, 2924–2932.
14 M. Zhou, Z. He, T. Wang, Y. Xu, W. Yu, B. Shi and K. Huang, *Microporous Mesoporous Mater.*, 2019, **274**, 245–250.
15 T. Xu, Y. He, Y. Qin, C. Zhao, C. Peng, J. Hu and H. Li, *RSC Adv.*, 2018, **8**, 4963–4968.
16 J. Dong, F. Xu, Z. Dong, Y. Zhao, Y. Yan, H. Jin and Y. Li, *RSC Adv.*, 2018, **8**, 19075–19084.
17 X. Li, L. Xie, X. Yang and X. Nie, *RSC Adv.*, 2018, **8**, 40321–40329.
18 C. Li, Y. He, L. Zhou, T. Xu, J. Hu, C. Peng and H. Liu, *RSC Adv.*, 2018, **8**, 41986–41993.
19 Z. Liu, C. Cao and B. Han, *J. Hazard. Mater.*, 2019, **367**, 348–355.
20 G. Li, H. Fang, D. Jiang and G. Zheng, *New J. Chem.*, 2018, **42**, 19734–19739.
21 L. Huang, M. He, B. Chen, Q. Cheng and B. Hu, *ACS Sustainable Chem. Eng.*, 2017, **5**, 4050–4055.
22 J. Fu, J. Zhu, Z. Wang, Y. Wang, S. Wang, R. Yan and Q. Xu, *J. Colloid Interface Sci.*, 2019, **542**, 123–135.
23 X. Zhu, S. An, Y. Liu, J. Hu, H. Liu, C. Tian, S. Dai, X. Yang, H. Wang and C. W. Abney, *AIChE J.*, 2017, **63**, 3470–3478.
24 Y. Hou, J. Sun, D. Zhang, D. Qi and J. Jiang, *Chem.–Eur. J.*, 2016, **22**, 6345–6352.
25 Q. Zhang, J. Yu, J. Cai, R. Song, Y. Cui, Y. Yang, B. Chen and G. Qian, *Chem. Commun.*, 2014, **50**, 14455–14458.
26 E. Haque, V. Lo, A. I. Minett, A. T. Harris and T. L. Church, *J. Mater. Chem. A*, 2014, **2**, 193–203.

27 Z. Qi, J. Yang, Y. Kang, F. Guo and W. Sun, *Dalton Trans.*, 2016, **45**, 8753–8759.
28 M. Guo, S. Liu, H. Guo, Y. Sun, X. Guo and R. Deng, *Dalton Trans.*, 2017, **46**, 14988–14994.
29 Y. Hui, C. Kang, T. Tian, S. Dang, J. Ai and C. Liu, *CrystEngComm*, 2017, **19**, 1564–1570.
30 J. D. Evans, K. E. Jelfs, G. M. Day and C. J. Doonan, *Chem. Soc. Rev.*, 2017, **46**, 3286–3301.
31 G. Zhang and M. Mastalerz, *Chem. Soc. Rev.*, 2014, **43**, 1934–1947.
32 T. Hasell and A. I. Cooper, *Nat. Rev. Mater.*, 2016, **1**, 16053.
33 S. J. Dalgarno, P. K. Thallapally, L. J. Barbour and J. L. Atwood, *Chem. Soc. Rev.*, 2007, **36**, 236–245.
34 J. D. Evans, C. J. Sumby and C. J. Doonan, *Chem. Lett.*, 2015, **44**, 582–588.
35 S. Huang, G. Jin, H. Luo and T. S. Andy Hor, *Chem.–Asian J.*, 2015, **10**, 24–42.
36 H. Kudo, R. Hayashi, K. Mitani, T. Yokozawa, N. C. Kasuga and T. Nishikubo, *Angew. Chem., Int. Ed.*, 2006, **45**, 7948–7952.
37 J. Tian, P. K. Thallapally, S. J. Dalgarno, P. B. McGrail and J. L. Atwood, *Angew. Chem., Int. Ed.*, 2009, **48**, 5492–5495.
38 J. R. Holst, A. Trewin and A. I. Cooper, *Nat. Chem.*, 2010, **2**, 915–920.
39 P. K. Thallapally, B. P. McGrail, S. J. Dalgarno, H. T. Schaef, J. Tian and J. L. Atwood, *Nat. Mater.*, 2008, **7**, 146–150.
40 E. Sanna, E. C. Escudero-Adan, A. Bauza, P. Ballester, A. Frontera, C. Rotger and A. Costa, *Chem. Sci.*, 2015, **6**, 5466.
41 T. H. Chen, W. Kaveevivitchai, A. J. Jacobson and O. S. Miljanic, *Chem. Commun.*, 2015, **51**, 14096–14098.
42 N. Giri, M. G. Del Popolo, G. Melaugh, R. L. Greenaway, K. Ratzke, T. Koschine, L. Pison, M. F. C. Gomes, A. I. Cooper and S. L. James, *Nature*, 2015, **527**, 216–220.
43 P. K. Thallapally, S. J. Dalgarno and J. L. Atwood, *J. Am. Chem. Soc.*, 2006, **128**, 15060–15061.
44 J. Guo, L. Yu and H. Yue, *React. Funct. Polym.*, 2019, **135**, 58–64.
45 H. Yue, J. W. Guo, S. Q. Fu, X. Li, W. Q. Wen, W. Jiang, R. Tong and M. Haranczyk, *Chem. Eng. J.*, 2018, **335**, 887–895.
46 G. Ji, Z. Yang, H. Zhang, Y. Zhao, B. Yu, Z. Ma and Z. Liu, *Angew. Chem., Int. Ed.*, 2016, **55**, 9685–9689.
47 D. Shetty, I. Jahovic, J. Raya, F. Ravaux, M. Jouiad, J.-C. Olsen and A. A. Trabolsi, *J. Mater. Chem. A*, 2017, **5**, 62–66.
48 P. K. Thallapally, L. Dobrzanska, T. R. Gingrich, T. B. Wirsig, L. J. Barbour and J. L. Atwood, *Angew. Chem., Int. Ed.*, 2006, **45**, 6506.
49 S. J. Dalgarno, P. K. Thallapally, J. Tian and J. L. Atwood, *New J. Chem.*, 2008, **32**, 2095–2099.
50 H. Kumari, L. Erra, A. C. Webb, P. Bhatt, C. L. Barnes, C. A. Deakyne, J. E. Adams, L. J. Barbour and J. L. Atwood, *J. Am. Chem. Soc.*, 2013, **135**, 16963–16967.
51 X. Zhao, D. Wang, C. Xiang, F. Zhang, L. Liu, X. Zhou and H. Zhang, *ACS Sustainable Chem. Eng.*, 2018, **6**, 16777.